STABILITY AND GRID DISPERSION OF THE P-SV 4TH-ORDER STAGGERED-GRID FINITE-DIFFERENCE SCHEMES

PETER MOCZO, JOZEF KRISTEK AND ERIK BYSTRICKÝ

Geophysical Institute, Slovak Academy of Sciences, Bratislava, Slovak Republic *

Summary: *Stability and grid dispersion in the P-SV 4th-order in space, 2nd-order in time, displacement-stress staggered-grid finite-difference scheme is investigated in the case of a homogeneous unbounded medium. All results, however, also apply to the velocity-stress and displacement-velocity-stress finite-difference schemes.*

Independent stability conditions for the P and S waves are obtained by exact separation of equations for the two types of waves.

Since the S-wave group velocity can differ from the actual velocity as much as 5% for the sampling ratio 1/5, commonly used in numerical modelling, the sampling of the minimum S wavelength by 6 grid spacings (with the velocity difference not larger than 2.5%) is recommended.

Grid dispersion is strongest for a wave propagating in a direction of a coordinate axis and weakest for a wave propagating along a plane diagonal.

Grid dispersion in the 4^{th}-order scheme for the sampling ratios $s = 1/5$ and $s = 1/6$ is smaller than grid dispersion in the 2^{nd}-order scheme for $s = 1/10$ and $s = 1/12$, respectively.

Keywords: finite-difference method, staggered-grid schemes, stability and grid dispersion

1. INTRODUCTION

The 4^{th}-order staggered-grid finite-difference (FD) schemes have been recently used in many numerical studies of earthquake ground motion and seismic wave propagation. Therefore, *Moczo et al. (2000b)* investigated stability and grid dispersion in the 3D 4^{th}-order staggered-grid displacement-stress, velocity-stress and displacement-velocity-stress FD schemes. Since 2D P-SV simulations still have not lost their importance and are frequently used in seismological studies, we present here systematic and detailed treatment of stability and grid dispersion in the P-SV 4^{th}-order displacement-stress staggered-grid FD scheme (4^{th}-order version of the scheme suggested by *Luo and Schuster, 1990*). Similarly as in the 3D case, all results are also valid for the velocity-stress (*Levander, 1988*) and displacement-velocity-stress (*Moczo et al., 2000a*) schemes.

Partial information on stability and grid dispersion in the P-SV FD schemes can be found in papers by *Virieux (1986)*, *Levander (1988)* and *Crase et al. (1992)*. *Virieux (1986)* shows stability condition and phase-velocity dispersion curves for his 2nd-order velocity-stress scheme. *Levander (1988)* presents stability condition and phase-velocity dispersion curves for his 4th-order velocity-stress scheme. Levander, however, did not obtain two simple independent equations leading to the P- and S-wave stability conditions. *Crase et al. (1992)* derived stability conditions for the P-SV case of an arbitrary order of approximation using a decomposition of the matrix scheme and a Fourier transform. They, however, do not show grid dispersion. Let us also mention the stability and grid dispersion analysis performed by *Rodrigues (1993)* for the 3D 8th-order displacement-stress scheme.

* Address: Dúbravská cesta 9, 842 28 Bratislava, Slovak Republic
(Fax: +421 7 5941 0626, E-mail: geofpemo@savba.sk)

Since we investigated the case of a homogeneous unbounded medium, the results and conclusions cannot be directly applied to media with free surface and material discontinuities. A separate additional analysis or numerical tests for such media is needed.

2. EQUATION OF MOTION AND THE P-SV 4TH-ORDER DISPLACEMENT-STRESS FINITE-DIFFERENCE SCHEME

Consider Cartesian coordinate system (x,z). Let density ρ and Lamé elastic coefficients λ and μ be functions of spatial coordinates x, z. Let displacement vector $\vec{u}(u,0,w)$, stress tensor $\tau_{\varepsilon\kappa}; \varepsilon,\kappa \in \{x,z\}$, and body force per unit volume $\vec{f}(f_x,f_z)$ be functions of x, z and time t. The equation of motion and Hooke's law for a perfectly elastic, inhomogeneous, isotropic medium are

$$\rho u_{tt} = \tau_{xx,x} + \tau_{xz,z} + f_x$$

$$\rho w_{tt} = \tau_{xz,x} + \tau_{zz,z} + f_z$$

and

$$\tau_{xx} = (\lambda + 2\mu)u_x + \lambda w_z$$

$$\tau_{zz} = \lambda u_x + (\lambda + 2\mu)w_z$$

$$\tau_{xz} = \mu(u_z + w_x) \tag{1}$$

where $u_{tt} = \partial^2 u / \partial t^2$, $\tau_{xx,x} = \partial \tau_{xx} / \partial x$, $u_x = \partial u / \partial x$ and so on. We can call equations (1) the displacement-stress formulation of the equation of motion.

Consider a 2D regular rectangular staggered spatial grid with a grid spacing h. Denote Δt a time step and $a = -\frac{1}{24}$ and $b = \frac{9}{8}$ coefficients of the 4th-order approximation of the first derivative. Let $U^m_{I,L}$ be a discrete approximation to $u^m_{I,L} = u(x_I, z_L, t_m)$ where I, L are spatial indices and m is a time index. Similarly, let W, T^{xx}, T^{zz}, T^{xz}, F^x, and F^z be discrete approximations to w, τ_{xx}, τ_{zz}, τ_{xz}, f_x, and f_z. For equations (1) we can construct an explicit, 4th-order in space, 2nd-order in time, displacement-stress staggered-grid FD scheme (see also Fig. 1):

$$U^{m+1}_{I,L+1/2} = 2U^m_{I,L+1/2} - U^{m-1}_{I,L+1/2} + (\Delta^2 t / \rho_{I,L+1/2}) F^{x,m}_{I,L+1/2} + \frac{\Delta^2 t}{h} \frac{1}{\rho_{I,L+1/2}} \times$$

$$\times \left[a\left(T^{xx,m}_{I+3/2,L+1/2} - T^{xx,m}_{I-3/2,L+1/2}\right) + b\left(T^{xx,m}_{I+1/2,L+1/2} - T^{xx,m}_{I-1/2,L+1/2}\right) \right.$$

$$\left. + a\left(T^{xz,m}_{I,L+2} - T^{xz,m}_{I,L-1}\right) + b\left(T^{xz,m}_{I,L+1} - T^{xz,m}_{I,L}\right) \right]$$

$$W^{m+1}_{I+1/2,L} = 2W^{m}_{I+1/2,L} - W^{m-1}_{I+1/2,L} + (\Delta^2 t / \rho_{I+1/2,L}) F^{z,m}_{I+1/2,L} + \frac{\Delta^2 t}{h} \frac{1}{\rho_{I+1/2,L}} \times$$

$$\times \left[a\left(T^{xz,m}_{I+2,L} - T^{xz,m}_{I-1,L}\right) + b\left(T^{xz,m}_{I+1,L} - T^{xz,m}_{I,L}\right) + a\left(T^{zz,m}_{I+1/2,L+3/2} - \right.\right.$$

$$\left. - T^{zz,m}_{I+1/2,L-3/2}\right) + b\left(T^{zz,m}_{I+1/2,L+1/2} - T^{zz,m}_{I+1/2,L-1/2}\right) \right] \qquad (2)$$

$$T^{xx,m}_{I+1/2,L+1/2} = \frac{1}{h}\{ (\lambda + 2\mu)_{I+1/2,L+1/2} [a\left(U^{m}_{I+2,L+1/2} - U^{m}_{I-1,L+1/2}\right) +$$

$$+ b\left(U^{m}_{I+1,L+1/2} - U^{m}_{I,L+1/2}\right)] + \lambda_{I+1/2,L+1/2} [a\left(W^{m}_{I+1/2,L+2} - \right.$$

$$\left. - W^{m}_{I+1/2,L-1}\right) + b\left(W^{m}_{I+1/2,L+1} - W^{m}_{I+1/2,L}\right)]\}$$

$$T^{zz,m}_{I+1/2,L+1/2} = \frac{1}{h}\{ \lambda_{I+1/2,L+1/2} [a\left(U^{m}_{I+2,L+1/2} - U^{m}_{I-1,L+1/2}\right) +$$

$$+ b\left(U^{m}_{I+1,L+1/2} - U^{m}_{I,L+1/2}\right)] + (\lambda + 2\mu)_{I+1/2,L+1/2} \times$$

$$\times [a\left(W^{m}_{I+1/2,L+2} - W^{m}_{I+1/2,L-1}\right) + b\left(W^{m}_{I+1/2,L+1} - W^{m}_{I+1/2,L}\right)]\}$$

$$T^{xz,m}_{I,L} = \frac{1}{h} \mu_{I,L} [a\left(U^{m}_{I,L+3/2} - U^{m}_{I,L-3/2}\right) + + b\left(U^{m}_{I,L+1/2} - U^{m}_{I,L-1/2}\right) +$$

$$+ a\left(W^{m}_{I+3/2,L} - W^{m}_{I-3/2,L}\right) + b\left(W^{m}_{I+1/2,L} - W^{m}_{I-1/2,L}\right)]$$

The 2nd-order scheme is obtained from the 4th-order scheme by inserting $a = 0$ and $b = 1$.

3. STABILITY CONDITION FOR AN UNBOUNDED HOMOGENOUS MEDIUM

The *von Neumann (1943)* method can be used to analyze stability of the FD scheme. Assume errors in U, W, T^{xx}, T^{zz}, and T^{xz} at $x = Ih$, $z = Lh$ and $t = m\Delta t$ in the form

$$e(U) = AE \ , \qquad e(W) = BE$$

$$e(T^{xx}) = C_1 E \ , \qquad e(T^{zz}) = C_2 E \ , \qquad e(T^{xz}) = C_3 E$$

$$E = \exp i(-\omega m\Delta t + k_x Ih + k_z Lh) \tag{3}$$

where ω is an angular frequency, k_x and k_z are the components of the wavenumber vector $\vec{k}$,

$$k_x = k\sin\delta \ , \qquad k_z = k\cos\delta \ , \qquad k = |\vec{k}| \tag{4}$$

and δ, an angle of the plane wave with respect to the z-axis (oriented vertically downward), is from interval

$$0 \le \delta \le \pi$$

Investigate propagation of the errors (3) in the grid. Inserting (3) into the FD scheme (2) leads, after some algebra that is analogous to that for the 3D case (*Moczo et al., 2000b*), to two independent equations

$$\sin\tfrac{1}{2}\omega\Delta t = \pm\frac{\Delta t}{h}\alpha\left(X^2 + Z^2\right)^{\frac{1}{2}} \tag{5}$$

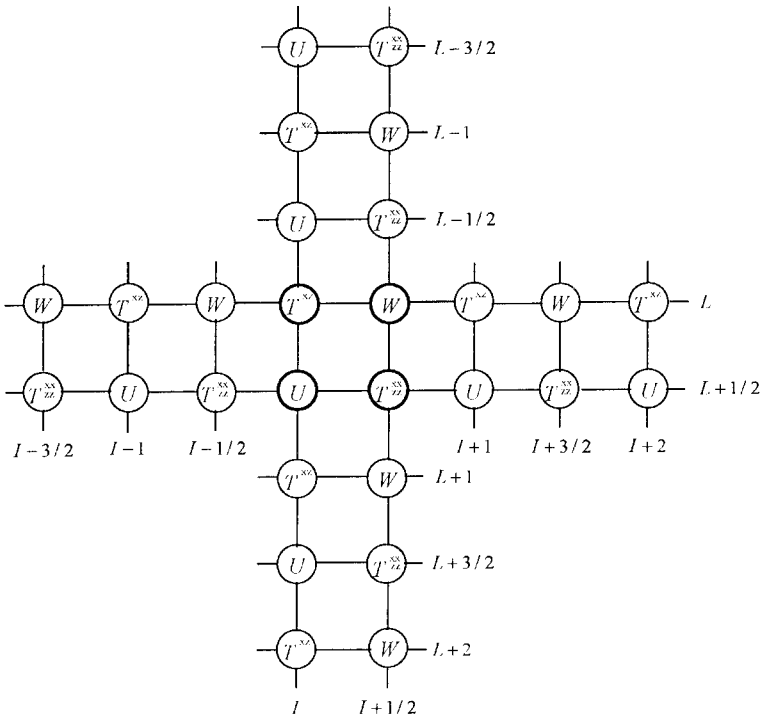

Fig. 1. Field variables entering the fourth-order displacement-stress finite-difference scheme.

$$\sin\tfrac{1}{2}\omega\Delta t = \pm\frac{\Delta t}{h}\beta\left(X^2+Z^2\right)^{\frac{1}{2}} \tag{6}$$

where α and β are the P- and S-wave velocities

$$\alpha^2 = \frac{\lambda+2\mu}{\rho}\,, \qquad \beta^2 = \frac{\mu}{\rho}$$

respectively, and

$$X = a\sin k_x\tfrac{3}{2}h + b\sin k_x\tfrac{1}{2}h$$

$$Z = a\sin k_z\tfrac{3}{2}h + b\sin k_z\tfrac{1}{2}h \tag{7}$$

Equation (5) implies a stability condition for the P wave:

$$\Delta t \le \frac{6}{7\sqrt{2}}\frac{h}{\alpha} \tag{8}$$

Similarly, equation (6) implies a stability condition for the S wave:

$$\Delta t \le \frac{6}{7\sqrt{2}}\frac{h}{\beta}$$

If both types of waves are generated and propagate in a medium, condition (8) for the P wave has to be taken as the joint stability condition since $\alpha > \beta$. Let us define a stability parameter p

$$p = \frac{7\sqrt{2}}{6}\frac{\Delta t}{h}\alpha \tag{9}$$

Then

$$p \le 1$$

It is easy to check, by inserting the errors given by eqs. (3) into the velocity-stress and displacement-velocity-stress schemes, that the obtained eqs. (5) and (6) as well as stability conditions are the same for the three schemes.

4. GRID DISPERSION

Both equations (5) and (6) can be (omitting the - sign) rewritten in the form

$$\frac{1}{2}\omega\Delta t = \arcsin\left[\frac{\Delta t}{h}c\left(X^2+Z^2\right)^{\frac{1}{2}}\right] \tag{10}$$

where c is either the P-wave velocity α or S-wave velocity β for the P or S wave, respectively. Since ω is the angular frequency in the grid,

$$\omega = 2\pi \frac{c^{grid}}{\lambda^{grid}} \tag{11}$$

where c^{grid} and λ^{grid} are the phase velocity and wavelength in the grid, equation (10) represents grid-dispersion relations for the P and S waves propagating in the grid.

Define, at a given frequency, a spatial sampling ratio s for the S wave and spatial sampling ratio s_P for the P wave as

$$s = \frac{h}{\lambda_S^{grid}} \qquad \text{and} \qquad s_P = \frac{h}{\lambda_P^{grid}} \tag{12}$$

If both types of waves are generated and propagate in a medium we have to adopt one joint spatial sampling ratio in order to compare the P- and S-wave dispersions. Due to $\lambda_S < \lambda_P$ at a given frequency, s has to be taken as an argument in relations for both the P and S waves. Obviously, a spatial sampling ratio s_P for the P wave is

$$s_P = \frac{s}{r} \tag{13}$$

where r is a velocity ratio

$$r = \frac{\alpha}{\beta} \tag{14}$$

Dividing equation (10) for the P wave and S wave by α and β, respectively, and inserting relations (4, 7, 11-14) we obtain the normalized grid-dispersion relations for the P and S waves in the form

$$\frac{\alpha^{grid}}{\alpha} = q\frac{\sqrt{2}}{\pi}\frac{r}{p\cdot s}\arcsin\left(\frac{1}{q\sqrt{2}}pF_\alpha\right) \tag{15}$$

$$\frac{\beta^{grid}}{\beta} = q\frac{\sqrt{2}}{\pi}\frac{r}{p\cdot s}\arcsin\left(\frac{1}{q\sqrt{2}}\frac{p}{r}F_\beta\right) \tag{16}$$

where

$$q = \frac{7}{6}$$

$$F_\eta = \{[a\sin(3\pi\varsigma\sin\delta)+b\sin(\pi\varsigma\sin\delta)]^2 + [a\sin(3\pi\varsigma\cos\delta)+b\sin(\pi\varsigma\cos\delta)]^2\}^{\frac{1}{2}}$$

and

$$\varsigma = \frac{s}{r} \qquad \text{if} \qquad \eta = \alpha \qquad \text{or} \qquad \varsigma = s \qquad \text{if} \qquad \eta = \beta$$

The grid-dispersion relations for the 2nd-order scheme are obtained by inserting $a = 0$, $b = 1$ and $q = 1$. The stability parameter p in the 2nd-order scheme is defined as

$$p = \sqrt{2}\frac{\Delta t}{h}\alpha \ , \qquad p \le 1 \ .$$

Note that both the P- and S-wave grid dispersions now depend on the velocity ratio $r = \frac{\alpha}{\beta}$ (and thus on the Poisson's ratio $\sigma = (2 - r^2)/[2(1 - r^2)]$). The dependence of the S-wave dispersion on the velocity ratio r was introduced by considering the P-wave stability condition (8) as a joint condition for both types of waves. The dependence of the P-wave dispersion on the velocity ratio r was introduced by considering the spatial sampling ratio s (for the S wave) as a joint argument for both types of waves.

The existence of the grid dispersion of the phase velocity implies the existence of the grid group velocity $c_{group}^{grid} = \partial\omega / \partial k$ and its dispersion. We obtain

$$\frac{\alpha_{group}^{grid}}{\alpha} = \frac{2(f_1\Gamma_1 + f_2\Gamma_2)}{\left[F - \left(\frac{6}{7\sqrt{2}}pF\right)^2\right]^{1/2}} \ , \qquad \frac{\beta_{group}^{grid}}{\beta} = \frac{2(f_1\Gamma_1 + f_2\Gamma_2)}{\left[F - \left(\frac{6}{7\sqrt{2}}\frac{p}{r}F\right)^2\right]^{1/2}} \tag{17}$$

where

$$f_1 = a\sin(3\pi\varsigma\sin\delta) + b\sin(\pi\varsigma\sin\delta)$$

$$f_2 = a\sin(3\pi\varsigma\cos\delta) + b\sin(\pi\varsigma\cos\delta)$$

$$\Gamma_1 = \sin\delta\left[a\frac{3}{2}\cos(3\pi\varsigma\sin\delta) + b\frac{1}{2}\cos(\pi\varsigma\sin\delta)\right]$$

$$\Gamma_2 = \cos\delta\left[a\frac{3}{2}\cos(3\pi\varsigma\cos\delta) + b\frac{1}{2}\cos(\pi\varsigma\cos\delta)\right]$$

$$F = f_1^2 + f_2^2$$

and

$$\varsigma = \frac{s}{r} \text{ in the case of } \frac{\alpha_{group}^{grid}}{\alpha} \qquad \text{or} \qquad \varsigma = s \text{ in the case } \frac{\beta_{group}^{grid}}{\beta} \ .$$

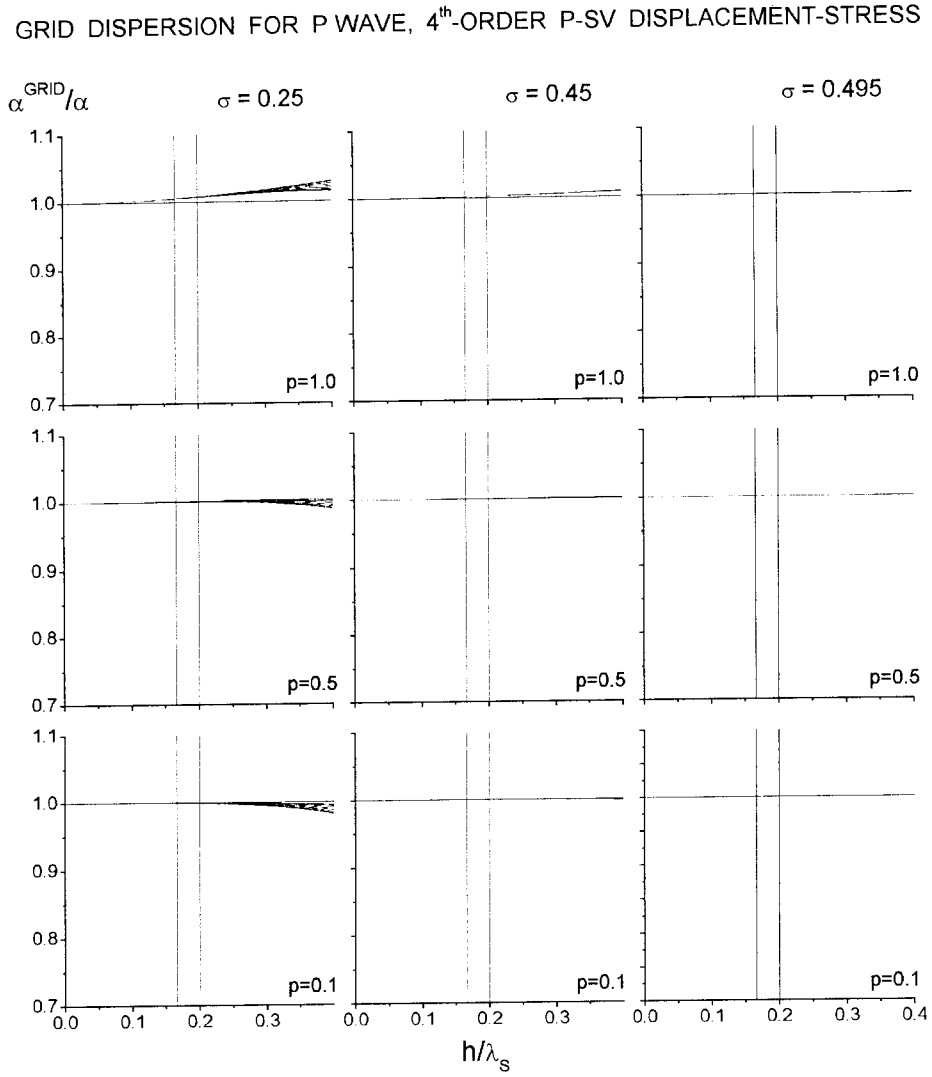

Fig. 2a. Grid-dispersion curves for the P wave propagating in 10 directions in a plane. Dispersion curves are shown for three values of the Poisson's ratio σ and three values of the stability parameter p. The three values of σ, 0.25, 0.45 and 0.495, correspond to α/β ratios of $\sqrt{3}$, 3.317 and 10, respectively. Two vertical lines indicate two values of the spatial sampling ratio ($s = h/\lambda_S$), $s = 1/6$ and $s = 1/5$, that are commonly used in numerical simulations. The horizontal line $\alpha^{grid}/\alpha = 1$ indicating the case of no grid dispersion is also shown for convenience.

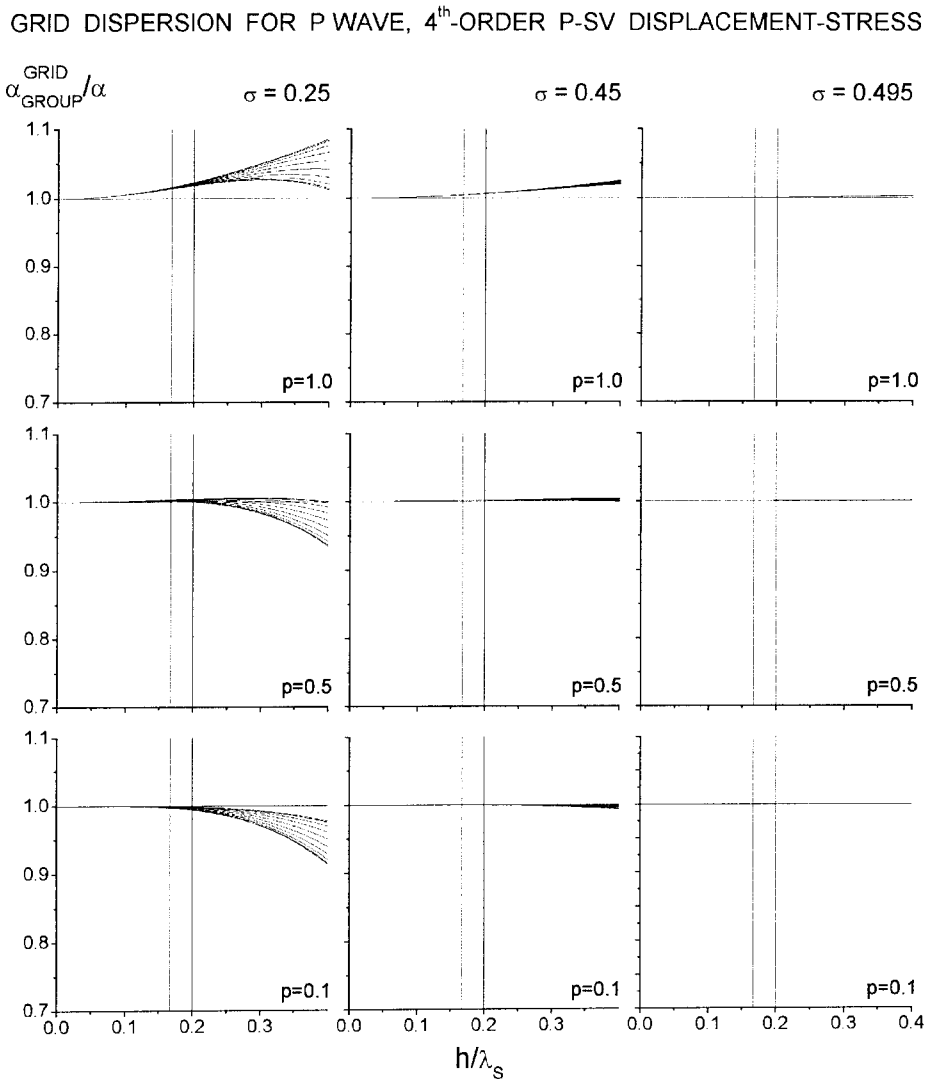

Fig. 2b. The same as in Fig. 2a but for the group velocity.

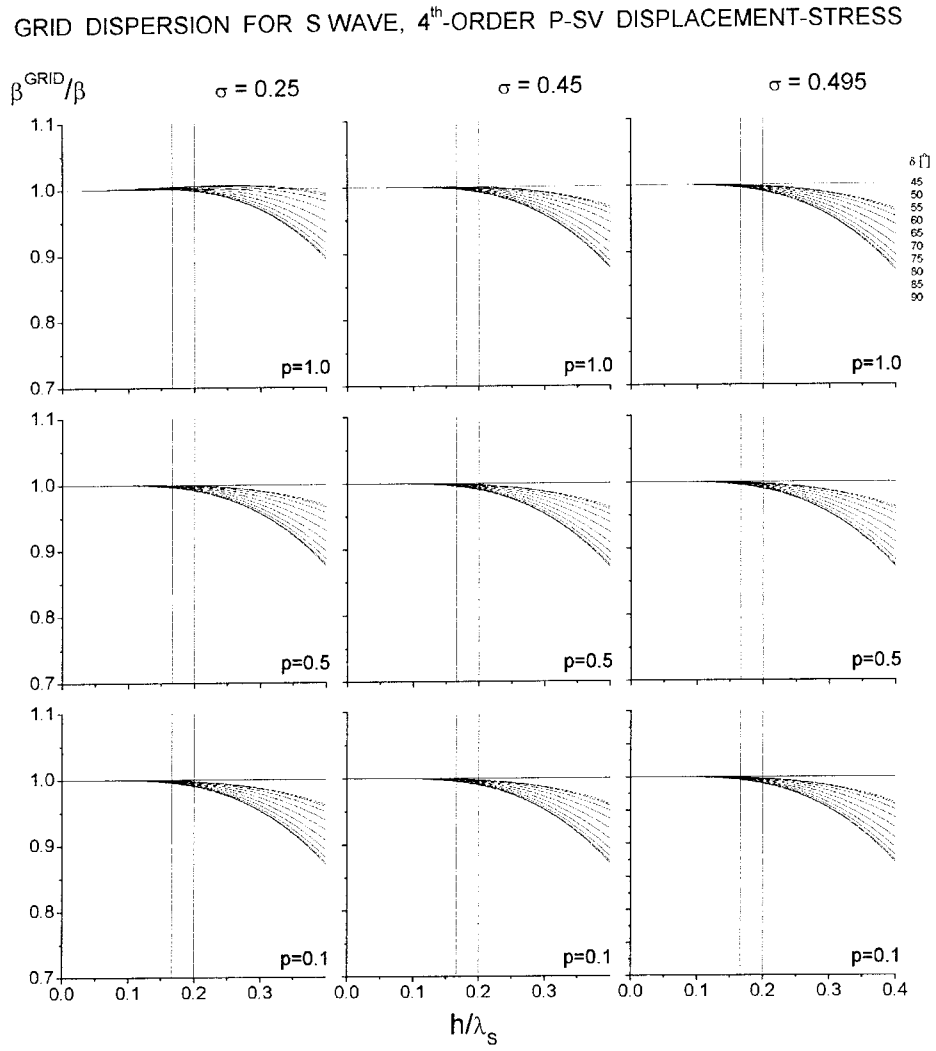

Fig. 3a. Grid-dispersion curves for the S wave propagating in 10 directions in a plane. Compare with Fig. 2a for the P wave.

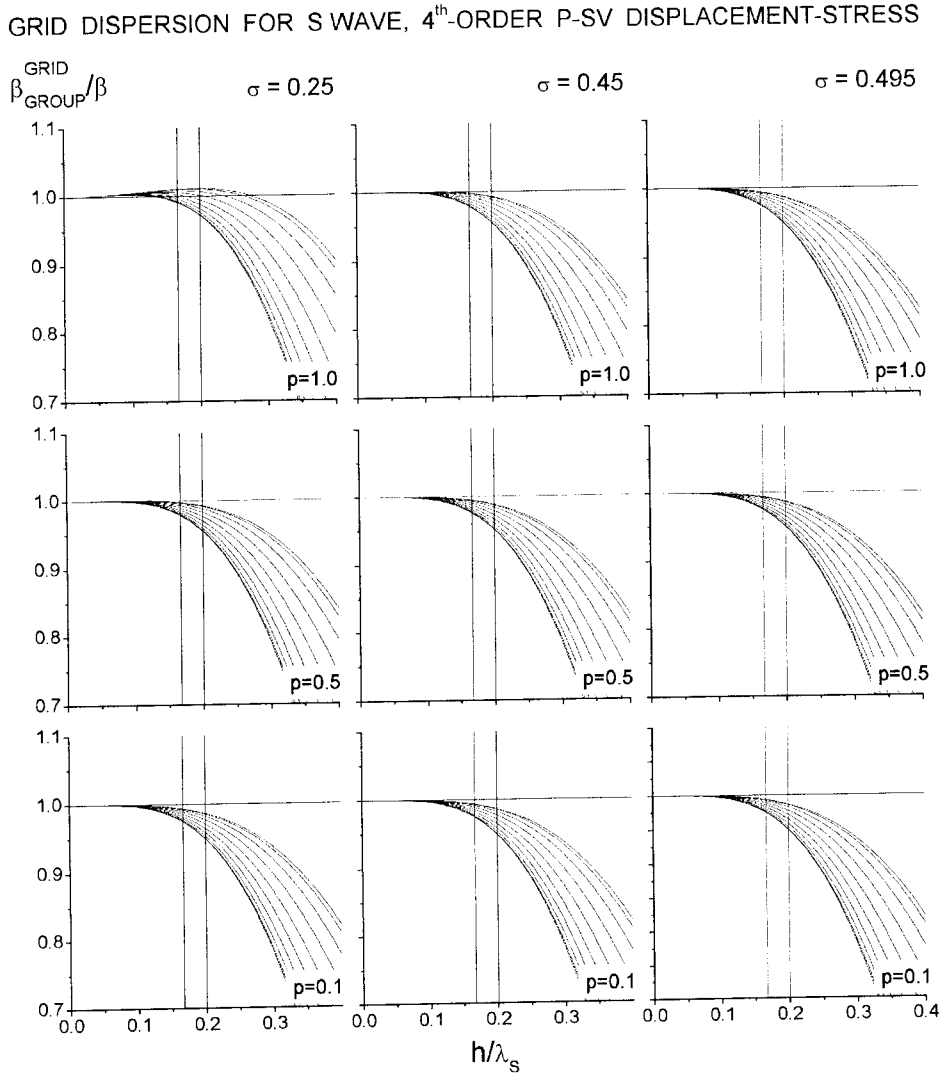

Fig. 3b. The same as in Fig. 3a but for the group velocity.

5. GRID DISPERSION - NUMERICAL RESULTS

Propagation in plane

In order to investigate scatter of the dispersion curves for different possible directions of propagation in plane we show first dispersion curves for the P and S waves propagating in ten directions defined by angle δ

$$\delta \in \{45°,50°,55°,60°,65°,70°,75°,80°,85°,90°\}$$

Fig. 2a shows the phase-velocity dispersion curves for the P wave for three values of the Poisson's ratio σ and three values of the stability parameter p. Analogously, Fig. 3a shows dispersion curves for the S wave. Two vertical lines shown for each set of the curves indicate two values of the spatial sampling ratio, $s = 1/6$ and $s = 1/5$, that are commonly used in numerical simulations. It is important to show dispersion for p values as low as 0.5 and 0.1. This is because in practical simulations a model of medium often consists of several layers and the maximum P-wave velocity in the model is 2 or more times, sometimes even 10 times, larger than the minimum P-wave velocity. Since the time step is determined by the maximum P-wave velocity, it is, say, 2 to 10 times smaller than that required by the layer with the minimum velocity. Correspondingly, an effective stability parameter p for a layer with the minimum velocity is as low as 0.5 to 0.1.

As expected, and similarly with the 3D case, due to a longer wavelength of the P wave propagation of the P wave is modeled by the FD scheme better than that of the S wave. Compared to the P wave, there is relatively considerable grid-dispersion anisotropy of the S wave.

For a given Poisson's ratio σ and direction of propagation, both α^{grid}/α and β^{grid}/β decrease with a decreasing value of the stability parameter p. Sensitivity of β^{grid}/β to the stability parameter p decreases with an increasing value of the Poisson's ratio σ. For a given direction of propagation and stability parameter p, β^{grid}/β decreases with an increasing Poisson's ratio σ.

For a given direction of propagation, the S-wave dispersion curves for all values of the Poisson's ratio σ are very close to each other in the case of the stability parameter $p = 0.1$. This, similarly as in the 3D case, is understandable if we examine a limit of β^{grid}/β for $p \to 0$. Dispersion relation (16) can be written as

$$\beta^{grid}/\beta = \psi \frac{r}{p} \arcsin\left(\chi \frac{p}{r}\right)$$

where the meaning of $\psi = \psi(s)$ and $\chi = \chi(s, \delta)$ is clear from relation (16). Then

$$\lim_{p \to 0} \left(\beta^{grid}/\beta\right) = \psi \cdot \chi$$

This explains why the dispersion curves (for a given direction of propagation) for p as low as 0.1 are so close to each other regardless of the value of the Poisson's ratio σ.

Majority of the displayed S-wave dispersion curves exhibit $\beta^{grid}/\beta < 1$. Thus, in majority cases, the grid dispersion causes delays of the S-wave arrivals. There are,

however, some curves, mainly for $\sigma = 0.25$, that exhibit $\beta^{grid}/\beta > 1$ at certain intervals of the sampling ratio s.

Table 1 shows minimum β^{grid} in % of β for two values of the sampling ratio s, $s = 1/5$ and $s = 1/6$, three values of the Poisson's ratio σ and two values of the stability parameter p. It is clear from Table 1 that for $s = 1/5$ and $s = 1/6$, β^{grid} does not differ from the actual velocity β more than, approximately, 0.9% and 0.5%, respectively. Consider, for example, $\beta = 300$ *m/s* and travel distance of 10000*m* that are reasonable values in large sedimentary basins or valleys. Then, the delays in the S-wave arrival caused by the grid dispersion are 0.303 sec and 0.168 sec for the sampling ratios $s = 1/5$ and $s = 1/6$, respectively.

Table 1. Minimum grid S-wave phase velocities β^{grid} in % of the actual velocity β

$s = 1/5$			
p	σ		
	0.25	0.45	0.495
1.0	99.733	99.150	98.959
0.5	99.132	98.989	98.941
0.1	98.943	98.938	98.936
$s = 1/6$			
p	σ		
	0.25	0.45	0.495
1.0	100.031	99.622	99.488
0.5	99.610	99.509	99.476
0.1	99.477	99.473	99.472

s – spatial sampling ratio; σ – Poisson's ratio; p – stability parameter

While there is practically no grid dispersion for the Poisson's ratio $\sigma = 0.495$ for the sampling ratios $s < 0.4$, $\alpha^{grid}/\alpha > 1$ at all directions of propagation for the stability parameter $p = 1.0$ and Poisson's ratios $\sigma = 0.25$ and $\sigma = 0.45$. The latter case means that the grid dispersion causes unphysical earlier P-wave arrivals. If necessary, and given relatively low sensitivity of β^{grid}/β to the stability parameter p, the earlier arrivals can be prevented by taking p as low as 0.5, i.e., by using half-value of the maximum possible time step Δt.

Fig. 2b shows dispersion curves of the P-wave group velocity for three values of the Poisson's ratio σ and three values of the stability parameter p. Analogously, Fig. 3b shows dispersion curves of the S-wave group velocity. What was said about the phase-velocity grid dispersion with respect to the Poisson's ratio σ and stability parameter p, is qualitatively also true about the group-velocity grid dispersion. An important difference is

considerably larger grid-dispersion anisotropy. Table 2 shows minimum β_{group}^{grid} in % of β for two values of the sampling ratio s, $s = 1/5$ and $s = 1/6$, three values of the Poisson's ratio σ and two values of the stability parameter p. It is clear from Table 2 that for $s = 1/5$ and $s = 1/6$, β_{group}^{grid} can differ from the actual velocity β, similarly as in the 3D case, as much as, approximately, 5% and 2.5%, respectively. Considering again the example with $\beta = 300$ *m/s* and travel distance of 10000*m*, the delays in the S-wave energy arrival caused by the grid dispersion are 1.754 sec and 0.877 sec for the sampling ratios $s = 1/5$ and $s = 1/6$, respectively. Clearly, taking 6 grid spacings per minimum wavelength of the S wave, i.e., $s = 1/6$, is better than taking only 5 grid spacings.

Finally, let us make a note on the grid dispersion for high values of the Poisson's ratio. It is clear from the figures that the grid velocities do not attain anomalous values for the Poisson's ratio approaching 0.5. In other words, they do not degrade. Thus, there is no indication of problems with liquids and solid-liquid interface.

Table 2. Minimum grid S-wave group velocities β_{group}^{grid} in % of the actual velocity β

$s = 1/5$			
p	σ		
	0.25	0.45	0.495
1.0	97.205	95.495	94.944
0.5	95.443	95.031	94.894
0.1	94.900	94.883	94.878
$s = 1/6$			
p	σ		
	0.25	0.45	0.495
1.0	99.087	97.872	97.476
0.5	97.835	97.538	97.440
0.1	97.444	97.432	97.428

s – spatial sampling ratio; σ – Poisson's ratio; p – stability parameter

Propagation in Two Distinct Directions

There are two distinct directions of propagation in the considered regular rectangular spatial grid – along a coordinate axis and coordinate-plane diagonal. Here we consider the x-axis ($\delta = 90°$) and the xz-plane diagonal ($\delta = 45°$). Figure 4 shows dispersion curves for the P wave propagating in the two directions for three values of the Poisson's ratio σ and four values of the stability parameter p. Analogously, Fig. 5 shows the dispersion curves for the S wave.

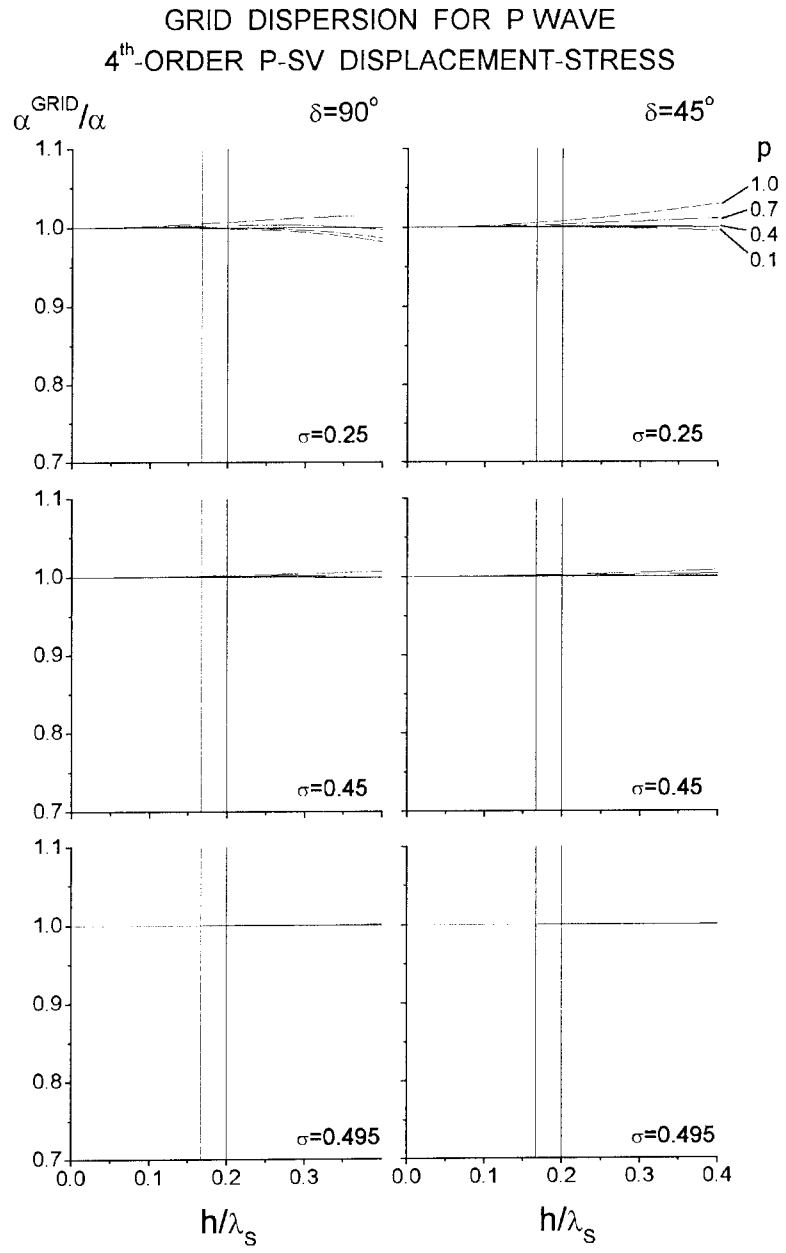

Fig. 4. Grid dispersion curves for the P wave propagating in the two distinct directions – along a coordinate axis and plane diagonal. Here we consider the x-axis ($\delta = 90°$) and plane diagonal determined by $\delta = 45°$. The dispersion curves are shown for three values of the Poisson's ratio σ and four values of the stability parameter p.

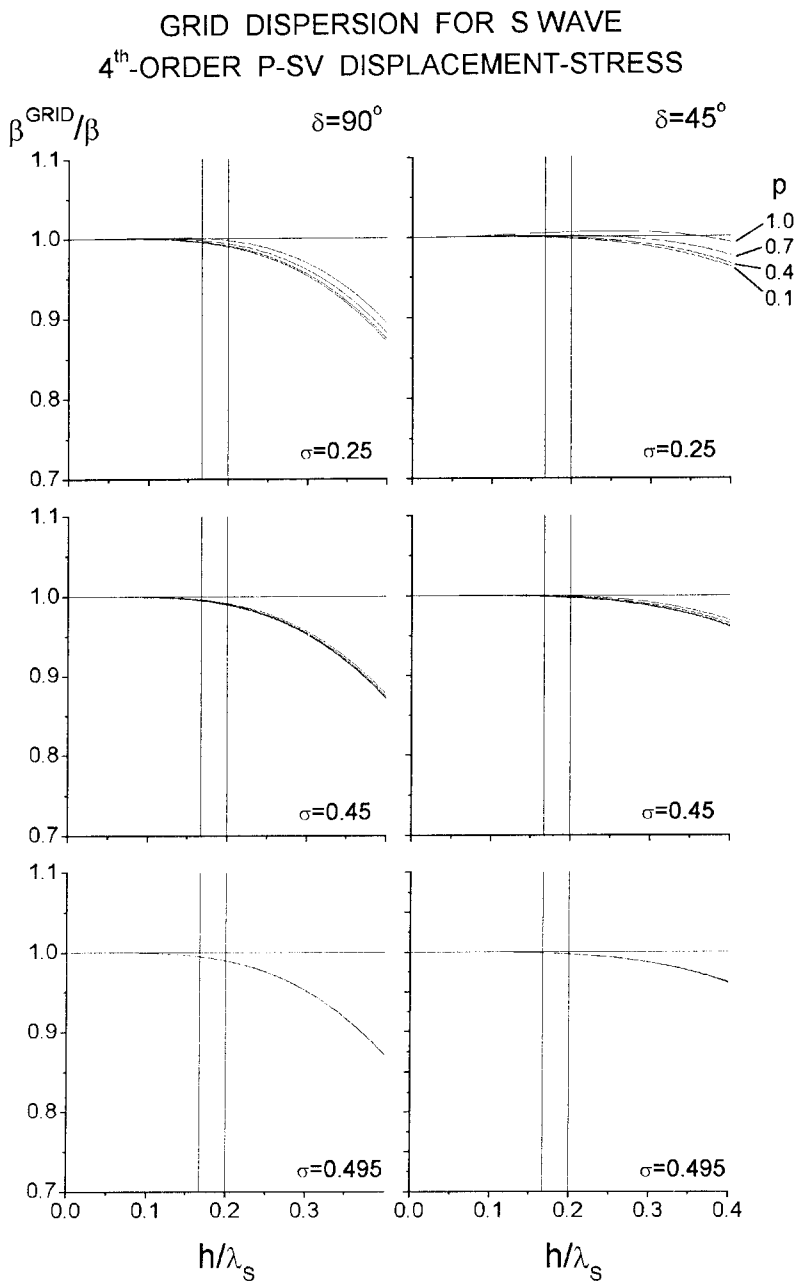

Fig. 5. The same as in Fig. 4 but for the S wave.

For given values of the spatial sampling ratio s , Poisson's ratio σ, and stability parameter p, c^{grid}/c (where c is α or β) is larger at the direction of the plane diagonal. Except the case of $\sigma = 0.25$ and $p = 1.0$, the scheme better models propagation in the direction of the plane diagonal compared to the direction of the coordinate axis. For a given type of wave, direction of propagation and value of the Poisson's ratio σ, c^{grid}/c decreases with decreasing value of the stability parameter p. For a given type of wave and direction of propagation, sensitivity of c^{grid}/c to the value of the stability parameter p considerably decreases as the value of the Poisson's ratio σ increases.

We can illustrate an effect of the grid dispersion on a plane S wave propagating in the direction of the x-axis ($\delta = 90°$). Consider a medium with $\beta = 300$ *m/s* and $\alpha = 1000$ *m/s*, i.e., $\sigma = 0.4505$. Let the time function of the wave be Gabor signal

$$s(t)=\exp\left\{-\left[\omega_p(t-t_s)/\gamma_s\right]^2\right\}\cos\left[\omega_p(t-t_s)+\theta\right].$$

Here, $\omega_p = 2\pi f_p$, $t \in <0, 2t_s>$, $f_p = 0.5$ Hz is predominant frequency, $\gamma_s = 11$ controls the width of the signal, $\theta = \pi/2$ is a phase shift, and $t_s = 0.45\gamma_s/f_p$. The predominant frequency of 0.5 Hz is a typical one in recent seismic ground motion modelling. The amplitude spectrum of the signal is shown in Fig. 6. The spectrum falls-off by three orders of magnitude from its maximum at the frequency of 0.74 Hz. Physically, this example is identical with that shown by *Moczo et al. (2000b)* for the 3D case. The difference is that here we do not propagate a plane wave in a 3D grid since we work only with a 2D grid assuming that propagation in our xz-plane is identical with propagation in any parallel xz-plane.

In Fig. 7 we show two cases. In the first one, a spatial sampling criterion is applied to a wavelength $\lambda_{0.5\ \mathrm{Hz}}$ at the predominant frequency. Two numerical solutions – one for 6 and one for 5 grid spacings per $\lambda_{0.5\ \mathrm{Hz}}$ – are shown together with the exact solution (middle panel in Fig. 7). An effect of the grid phase-velocity dispersion is shown on the left-hand side (signals) while an effect of the grid group-velocity dispersion is shown on the right-hand side of the figure (envelopes). First, compare the numerical solution for 5 grid spacings per $\lambda_{0.5\ \mathrm{Hz}}$ with the exact one. Both the signal and envelope of the numerical solution are distorted and delayed with respect to the exact solution. The delays of the maximum amplitudes of the signal and envelope are approximately 10% larger than delays simply predicted for the predominant frequency from the corresponding values of the grid phase and group velocities for a given travel distance. This is due to the effect of the spectral content of the Gabor signal at frequencies higher than the predominant frequency (see Fig. 6).

Compare now the two solutions with the numerical one for 6 grid spacings per $\lambda_{0.5\ \mathrm{Hz}}$. We can see in Fig. 7 that the delays of the maximum amplitudes of the signal and envelope (with respect to the exact solution) are approximately twice smaller compared with those for 5 grid spacings per $\lambda_{0.5\ \mathrm{Hz}}$.

The lower part of Fig. 7 compares the exact solution with two numerical ones for 5 and 6 grid spacings applied to $\lambda_{0.74\ \mathrm{Hz}}$. As expected, delays due to the grid dispersion are much smaller compared with those in the above case.

An important fact in both cases is that using 6 grid spacings per a wavelength instead of 5 grid spacings decreases delays in phase and energy arrivals approximately twice.

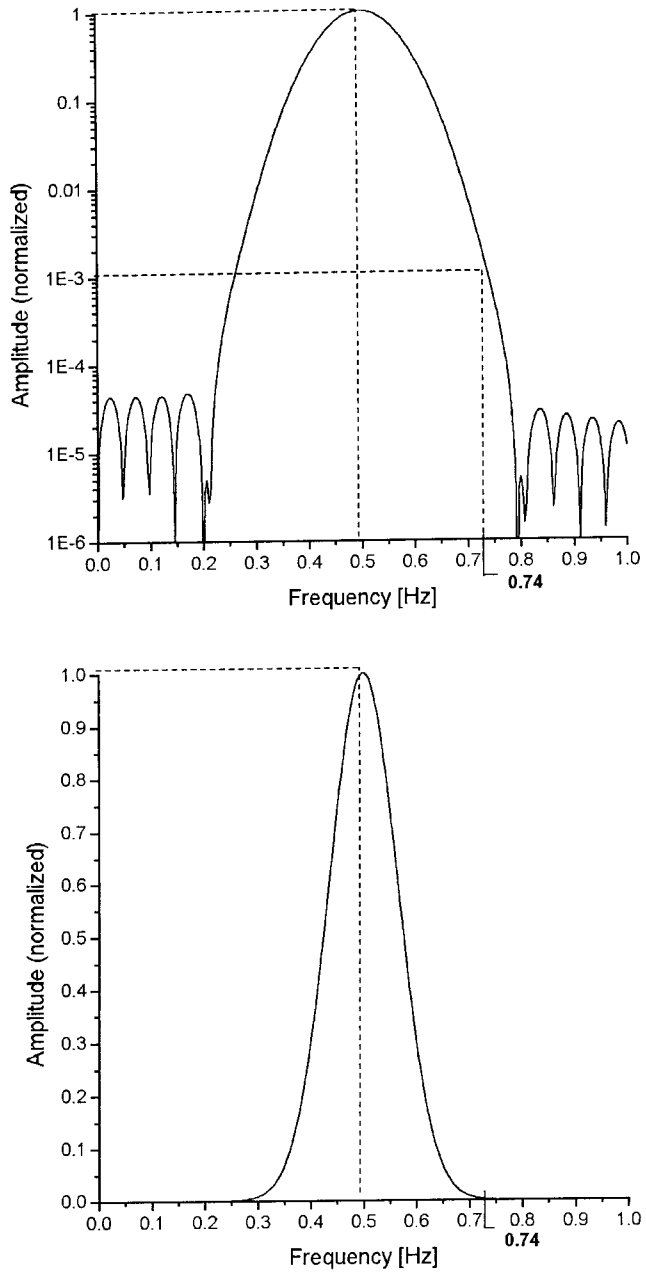

Fig. 6. Amplitude Fourier spectrum of Gabor signal used in the example of an effect of the grid dispersion on a plane S wave propagation.

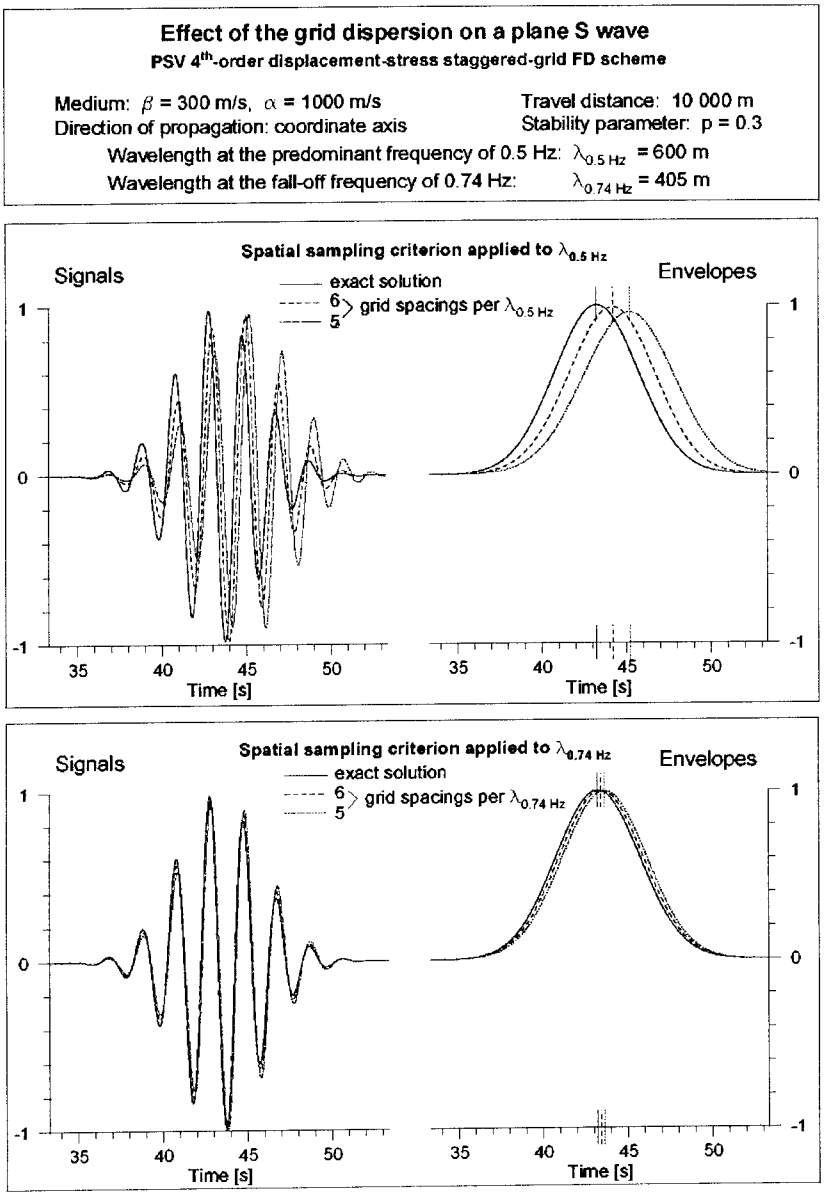

Fig. 7. Example of an effect of the grid dispersion on a plane S wave propagation in a grid in two cases. First, a spatial sampling criterion is applied to the wavelength at the predominant frequency of the signal. Second, a spatial sampling criterion is applied to the wavelength at the frequency at which the amplitude spectrum falls-off by three orders of magnitude from its maximum value (see Fig. 6). All numerical solutions are compared with the exact one.

The example also indicates that it is not enough to apply a spatial sampling criterion to a wavelength corresponding to a predominant frequency if the spectral content at higher frequencies of a signal is non-negligible.

Finally, let us note that the numerical solutions in Fig. 7 are very close to those shown by *Moczo et al. (2000b)* for the 3D case.

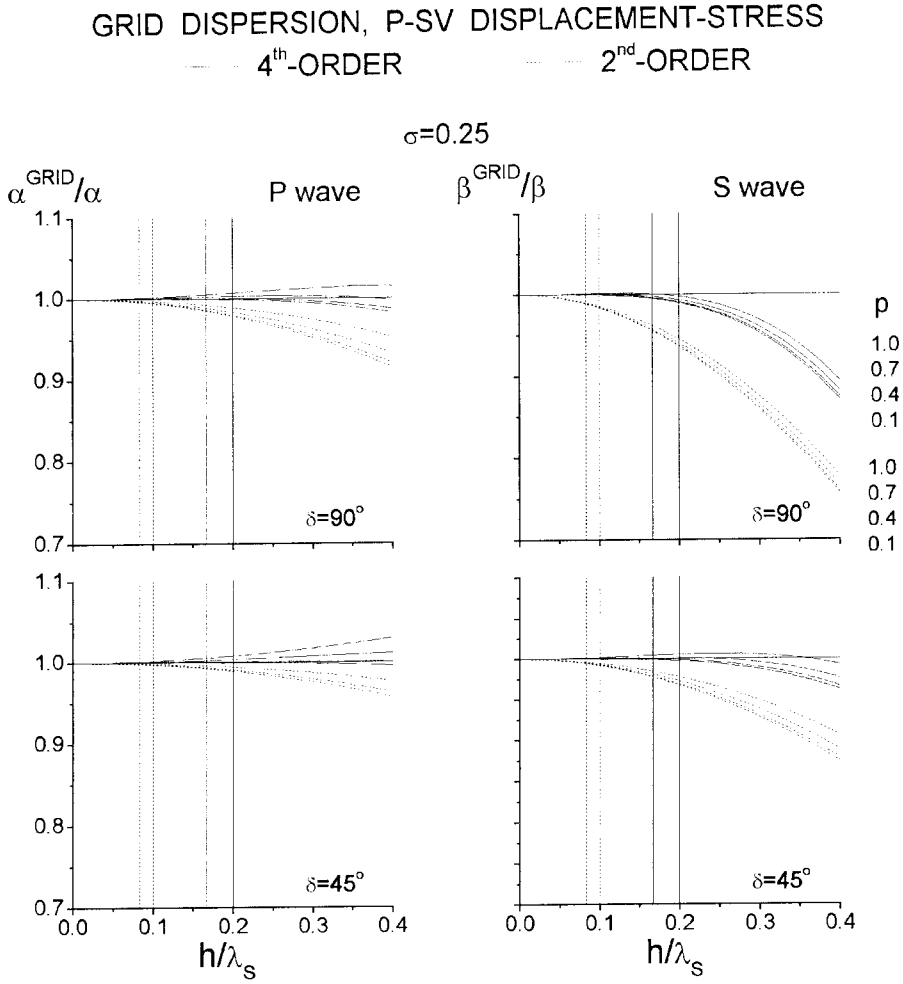

Fig. 8. Comparison of the grid dispersion in the 4th-order and 2nd-order FD schemes. The dispersion curves are shown for the P and S waves propagating in the two distinct directions for the Poisson's ratio $\sigma = 0.25$ and four values of the stability parameter p. Four vertical lines indicate four values of the spatial sampling ratio – $s = 1/12$, $s = 1/10$ and $s = 1/6$, $s = 1/5$ – that are commonly used in numerical simulations by the 2nd-order and 4th-order FD schemes.

Comparison with the 2nd-order Scheme

Grid dispersion in the 4th- and 2nd-order schemes is compared in Fig. 8. Dispersion for the two distinct directions of propagation is illustrated. Similarly as in the 3D case, the difference between the two orders of approximation is significant. The 2nd-order scheme models both the P- and S-wave propagation much worse than the 4th-order scheme does.

There is one interesting exception in the 2nd-order scheme. It is easy to see from eq. (15) that for $\delta = 45°$ (plane diagonal) and $p = 1.0$, $\alpha^{grid}/\alpha = 1$ for all values of the spatial sampling ratio s, i.e., there is no grid dispersion of the P wave propagating in the direction of a plane diagonal at the stability limit. This is illustrated by a missing dispersion curve in the bottom left set of the curves in Fig. 8 (the dispersion curve coincides with the horizontal line $\alpha^{grid}/\alpha = 1$).

Another interesting feature of the grid dispersion in the 2nd-order scheme is that $c^{grid}/c < 1$ (where c is α or β), i.e., there are no grid-dispersion related earlier arrivals.

6. CONCLUSIONS

Stability and grid dispersion in the P-SV 4th-order in space, 2nd-order in time, displacement-stress staggered-grid finite-difference scheme were analyzed in the case of a homogeneous medium.

Exact separation of equations for the P and S waves leads to the independent stability conditions for the two types of waves.

Considering the P-wave stability condition as a joint stability condition, and the spatial sampling of the S wavelength at a given frequency as an argument in both dispersion relations, we consistently investigated the P- and S-wave grid dispersion.

Due to larger wavelength of the P wave, propagation of the P wave is modeled by the FD scheme better than that of the S wave. Compared to the P wave, there is considerable grid-dispersion anisotropy of the S-wave phase and mainly group velocity. Grid dispersion is strongest for a wave propagating along a coordinate axis and weakest for a wave propagating in the direction of a plane diagonal.

The phase velocity β^{grid} does not differ from the actual velocity β more than, approximately, 0.9% and 0.5% for the spatial sampling ratios $s = 1/5$ and $s = 1/6$, respectively. However, the group velocity β^{grid}_{group} can differ from β as much as 5% for the spatial sampling ratio $s = 1/5$ while it is 2.5% for $s = 1/6$. Therefore, we recommend to sample a minimum S wavelength by 6 grid spacings (instead of 5 that is prevailing practice).

The 4th-order scheme models wave propagation much better than the 2nd-order scheme. Moreover, grid dispersion of the S wave in the 2nd-order scheme for the sampling ratios $s = 1/10$ and $s = 1/12$ is larger than grid dispersion in the 4th-order scheme for $s = 1/5$ and $s = 1/6$, respectively.

Acknowledgments: This work was supported in part by Grant No. 2/5131/98, VEGA, Slovak Republic, and INCO-COPERNICUS Grant PL963311. Numerical computations were performed on SGI Origin 2000 in the Computing Center of the Slovak Academy of Sciences.

Manuscript received: 10 January 2000; Revisions accepted: 15 June 2000

References

Crase, E., Ch. Wideman, M. Noble, and A. Tarantola (1992). Nonlinear elastic waveform inversion of land seismic reflection data, *J. Geophys. Res.* **97**, 4685-4703.

Levander, A. (1988). Fourth-order finite-difference P-SV seismograms, *Geophysics* **53**, 1425-1436.

Luo, Y. and G. Schuster (1990). Parsimonious staggered grid finite-differencing of the wave equation, *Geophys. Res. Let.* **17**, 155-158.

Moczo, P., J. Kristek, and E. Bystrický (2000a). Efficiency and optimization of the 3D finite-difference modeling of seismic ground motion. *J. Comp. Acoustics*, in press.

Moczo, P., J. Kristek, and L. Halada (2000b). 3D 4th-Order Staggered-Grid Finite-Difference Schemes: Stability and Grid Dispersion. *Bull. Seism. Soc. Am.*, **90**.

Rodrigues, D. (1993). Large scale modeling of seismic wave propagation. Doctoral Degree Thesis. Ecole Centrale Paris, 112 pp.

Virieux, J. (1986). P-SV wave propagation in heterogeneous media: velocity-stress finite-difference method, *Geophysics*, **51**, 889-901.

von Neumann, J. (1943). Mathematische Grundlagen der Quantenmechanik, Dover, New York.